

Efficient Synthesis and Wetting Characteristics of Amphiphilic Galactose–PLA Block Copolymers: A Potential Additive for the Accelerated Biodegradation of Micro- and Nanoplastics

Lisa-Cathrin Leitner, Rika Schneider, Thomas Steiner, Martina H. Stenzel, Ruth Freitag,* and Andreas Greiner*

This publication is dedicated to Prof. Brigitte Voit on the occasion of her 60th birthday

The contamination of wastewater by microplastic particles (MPs) is an unresolved environmental problem. In order to resolve this problem, a concept is developed for the microbial remediation of MPs. To realize this concept, degradable block copolymers are required, which adhere on MP surfaces and contain segments of carbohydrate moieties (here galactose) for the attraction of degrading microbes and accelerated biofilm formation. Therefore, in this study, a versatile synthesis route for amphiphilic carbohydrate block copolymers from poly(D,L-lactic acid) (PLA) and galactose moieties is presented. The properties of the block copolymers are investigated by thermal analysis, as well as regarding their colloidal properties, their adhesion behavior on MP surfaces, and their potential for support of microbial growth (using *Lactococcus lactis*).

1. Introduction

The contamination with microplastic debris is an emerging environmental problem.^[1] Microplastic particles (MPs) are defined as polymer particles with a size of <5 mm.^[2] MP can have complex shapes (e.g., spherical, fibrous, and irregular) and have different chemical compositions.^[3] Primary and secondary MPs are known. Primary MPs are produced intentionally for various technical uses, e.g., in cosmetics, while secondary MPs are formed by degradation processes from larger plastic particles.^[4] Aquatic systems (e.g., oceans,^[5] rivers,^[6] and lakes^[7]), soil,^[8] and the atmosphere^[9] are increasingly contaminated by MPs.

Various strategies were developed in order to remove existing MP contamination from the environment with the focus mostly on aquatic systems.^[10] The major strategies for the removal of MPs from aquatic systems are based on filtration, coagulation, and chemical/enzymatic degradation. Currently, physical removal is the most popular strategy, but such strategies become less suited as the particles become smaller. Bioremediation strategies using bacterial or fungal degradation currently are still in a premature state. However, the feasibility of such bioremediation strategies has been proposed. For example, fungal degradation of polyethylene MP was found with marine fungi.^[11] Bacterial degradation of macroscopic samples of poly(ethylene terephthalate) (PET) was achieved with a newly identified strain named *Ideonella sakaiensis* 201-F6, which expresses the catabolic enzyme PETase.^[12] Periphytic biofilms were utilized for the degradation of PET.^[13] The rate of degradation by the biofilms was increased by addition of glucose. All these promising approaches also show that further conditioning is required in order to achieve fast, complete, and selective degradation of MPs by microbes. The degradation of MPs in wastewater plants is of particular interest in this context.


In order to trigger microbial degradation of MPs in wastewater plants, we consider a concept based on the addition of hydrophobic poly(D,L-lactic acid) (PLA) block copolymers with hydrophilic galactose moieties. The basic working hypothesis is that

L.-C. Leitner, R. Schneider, A. Greiner
Macromolecular Chemistry and Bavarian Polymer Institute, University of Bayreuth

Universitätsstraße 30
Bayreuth 95440, Germany
E-mail: andreas.greiner@uni-bayreuth.de

T. Steiner, R. Freitag
University of Bayreuth
Process Biotechnology
Universitätsstraße 30
Bayreuth 95440, Germany
E-mail: ruth.freitag@uni-bayreuth.de

M. H. Stenzel
School of Chemistry
University of New South Wales
Sydney, NSW 2052, Australia

 The ORCID identification number(s) for the author(s) of this article can be found under <https://doi.org/10.1002/macp.202100431>

© 2022 The Authors. Macromolecular Chemistry and Physics published by Wiley-VCH GmbH. This is an open access article under the terms of the Creative Commons Attribution License, which permits use, distribution and reproduction in any medium, provided the original work is properly cited.

DOI: 10.1002/macp.202100431

such an amphiphilic block copolymer will deposit on MP particles. The galactose-containing blocks will attract microbes as a potential food source and thereby trigger the biofilm formation, which finally leads to the microbial metabolization of the MPs with suitable microbes in the biofilm. PLA was selected as a hydrophobic block as it is well known to be biodegradable in the environment.^[14] The carbohydrate galactose was selected as carbohydrates are well-known substrates for microbes. The synthesis of PLA block copolymers with galactose moieties is possible by reversible addition-fragmentation chain-transfer (RAFT) polymerization as recently demonstrated by the Stenzel group.^[15] For the realization of the concept of the block copolymer triggering biofilm formation on MPs in waste water, efficient synthesis of the educts for the block copolymers and knowledge about their colloidal properties are essential first steps. Both aspects will be discussed in this contribution along with the important question whether microbes are attracted by and do digest the polymer-bound galactose moieties. We have utilized an assay with *Lactocaseibacillus zeae* as model organism for the investigation of this crucial aspect. It should be emphasized, that *L. zeae* cannot digest any plastics but serves in this study for the investigation of the microbial metabolizability of the block copolymers, which is a crucial precondition for the success of the concept.

2. Results and Discussion

2.1. Synthesis of the Block Copolymer Poly-D,L-Lactide-co-Poly(6-O-Acryloyl-R-D-Galactopyranose)

The reaction pathway for the synthesis of the galactose block copolymers is displayed in **Scheme 1**. First, the RAFT reagent **5** was synthesized, which served as an initiator for the ring-opening polymerization (ROP) of LA. According to a previously published procedure,^[15] the RAFT-functionalized PLA block **8** was used as a macroinitiator for the polymerization of the vinyl-galactose (GA) **12**, which finally resulted in the PLA-*b*-PALpGP **14**. In detail, the RAFT agent **5** was synthesized by the reaction of mercaptoethanol **1** and carbon disulfide **2** in attendance of potassium triphosphate **4**. After 10 min, benzyl bromide **3** was introduced and stirred for 1 h following a previous published procedure.^[16] The chemical structure and purity of **5** were confirmed by ¹H-NMR spectroscopy (Figure S1, Supporting Information). **5** was carried out for the termination in the ROP of **6** (LA), which was initiated by di-azabicycloundecen (**7** DBU). The ROP was proceeded at room temperature (rt) and with a reaction time of only 7 min to yield 95% (based on the initial monomer mass) of the PLA macroinitiator **8**. Gel permeation chromatography (GPC) of **8** showed a unimodal molecular weight distribution, with an apparent number average molecular weight of $M_{n,app} = 24.000 \text{ g mol}^{-1}$ ($\mathcal{D} = 1.16$) (**Figure 1**). The ¹H-NMR showed the characteristic peaks of PLA. Based on the peaks that can be assigned to **8**, a molecular weight of $16.100 \text{ g mol}^{-1}$ can be calculated (Figure S2, Supporting Information).

For the block copolymerization, the protected galactose molecule was provided with a polymerizable double bond **12**. Therefore, α -D-galactopyranose **10** was reacted with acryloyl chloride **9** in the presence of triethyl amine **11** in a very short reac-

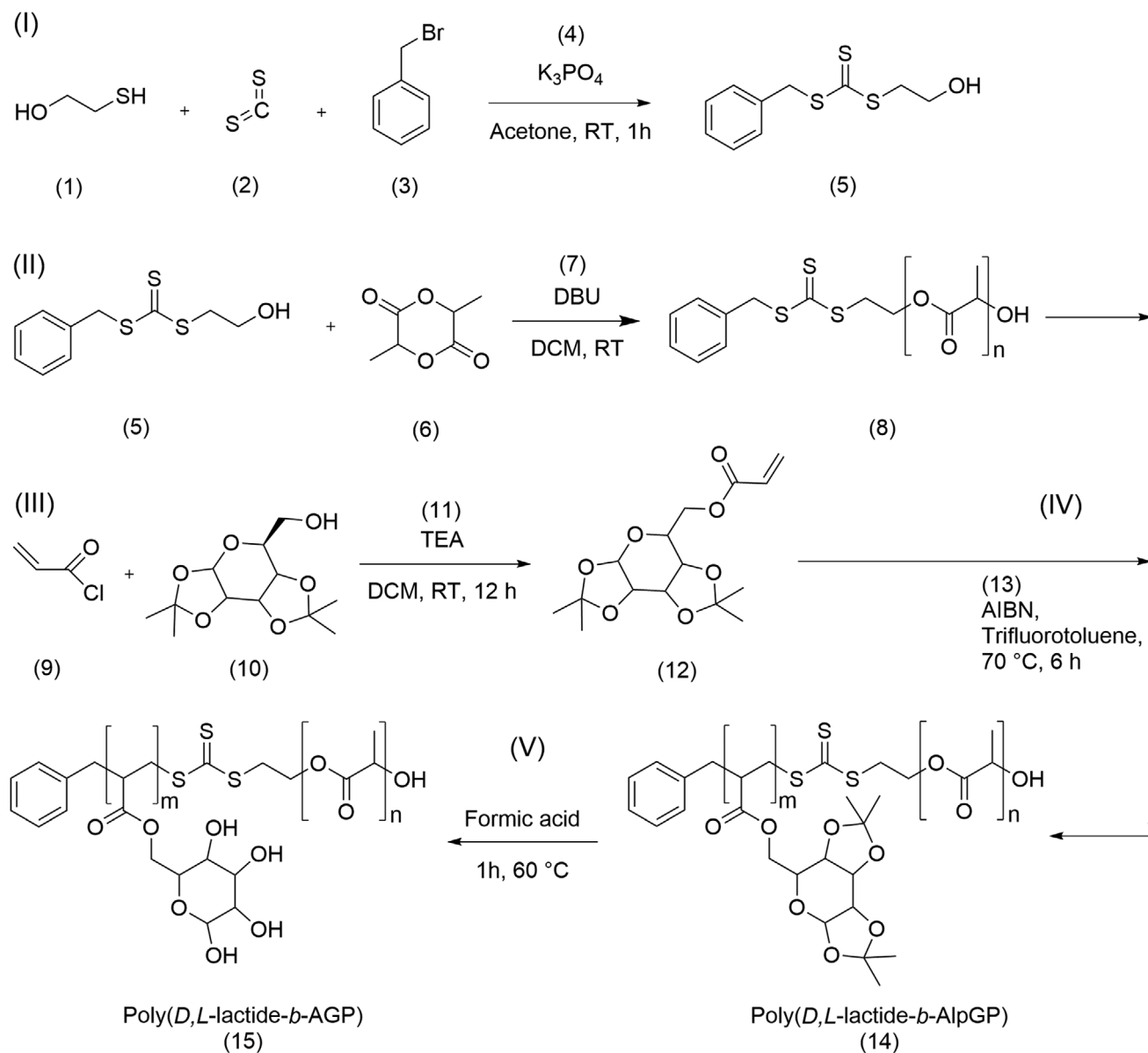
tion time. High purity of **12** was achieved even without column chromatography. The obtained monomer **12** (Figure S3, Supporting Information) was polymerized by RAFT polymerization with **8** and **13** as an initiator. The GPC measurement of **14** showed also a unimodal molecular weight distribution, with an apparent number average molecular weight of $M_{n,app} = 31.000 \text{ g mol}^{-1}$ ($\mathcal{D} = 1.42$) (Figure 1). This proves that the polymerization was successful. The low-molecular-weight tailing in the block copolymer can be assigned to the fraction of chains, which is formed as a result of the azobis-isobutyronitrile (AIBN) initiated step. This small fraction is not able to form block copolymers and will eventually be terminated. Some broadening might also be the result of incomplete chain extension of **8**.^[17] The galactose block in the polymer is therefore about 7.000 g mol^{-1} .

Infrared spectroscopy showed that the deprotection of **14** was efficient (**Figure 2**). While the carbonyl vibrations remain unchanged, the deprotected polymer **15** shows in the IR spectra a broad signal at 3400 cm^{-1} (Figure 2), which proofs the successful deacetalization and formation of hydroxyl groups.

The ¹H-NMR spectra of **14** and **15** show the characteristic signals for PLA as well as those of galactose (**Figure 3A,B**). The molecular weight of the sugar block can be calculated by relating the integrals of the peaks from PLA and the sugar (Figure 3A). As the PLA block has 220 repeat units (Figure S2, Supporting Information), 73 repeat units are obtained for the sugar block and thus the polymer with the composition PLA₂₂₀-*b*-PALpGP₇₃ is obtained

The signals of the spectra of **12** and **14** match each other, and the signals between 6.39 and 5.80 ppm belonging to the vinyl groups of the monomer have vanished (Figure S3, Supporting Information). In addition, the protective groups of **14** are no longer detectable in the spectrum of **15** (Figure 3B). We conclude that the deprotection was near quantitative.

14 shows a two-stage thermal degradation, with the first stage mainly degrading PLA and the second stage degrading the galactose block (Figure S4, Supporting Information). The first T_{max} is at $345 \text{ }^\circ\text{C}$ and within the first stage almost 76% of the mass of the polymer is degraded. In the second step with a T_{max} of $433 \text{ }^\circ\text{C}$, 13% of the mass is degraded. **15** loses 3% of its mass at $100 \text{ }^\circ\text{C}$. This results because of many hydroxyl groups in **15**, which are released as water vapor. Subsequently, there are several degradation steps that occur via rearrangements in the sugar residues.^[18] The largest degradation step comes from the PLA. In the differential scanning calorimetry (DSC) measurements, the glass transition temperature (T_g) values of PLA and of the galactose block are still visible (Figure S5, Supporting Information). In the measurement of **15**, the T_g of PLA is $62 \text{ }^\circ\text{C}$ and that of AlpGP is $108 \text{ }^\circ\text{C}$. Comparing the values with those of **14** shows that the T_g of PLA at $53 \text{ }^\circ\text{C}$ is slightly lower than that of **14**. However, this is due to the higher heating rate during the measurement. More striking is the T_g of acryloyl-galactopyranose (AGP), which is now $152 \text{ }^\circ\text{C}$ and thus 30% higher than the T_g of **14**. Since there are many hydroxide groups in **14** that form hydrogen bridges, the T_g in **15** increases to $152 \text{ }^\circ\text{C}$. **14** and **15** are amorphous as confirmed by wide-angle X-ray scattering (WAXS, Figure S6, Supporting Information). The signals are in the range of 7° – 25° and agree with those of amorphous PLA (**Table 1**).^[19]



Scheme 1. Reaction schemes from I) the synthesis of the RAFT reagent, II) the ring-opening polymerization of *D,L*-lactic acid, III) the synthesis of the 1,2:3,4-di-*O*-isopropylidene-6-*O*-acryloyl- α -*D*-galactopyranose, and IV) the RAFT reaction, which leads to the block-copolymer PLA-*b*-PAIpGP. V) After deprotection, the polymer PLA₂₂₀-*b*-PAGP₇₃ was obtained.

2.2. Formation of Micelles

The potential amphiphilic properties of **15** constitute an important precondition for intended adherence of **15** on MP surfaces. Therefore, we investigated the basic colloidal properties of **15** in aqueous environment starting from a solution of **15** in an organic solvent. **15** was first dissolved in dimethyl sulfoxide (DMSO). The addition of water to the DMSO solution of **15** initiated phase separations indicated by the turbidity of the mixture (Figure S7, Supporting Information), which is most likely due to the formation of micelles. The micelle formation was confirmed by dynamic light scattering (DLS) after removal of the DMSO by dialysis. The re-

sulting aqueous dispersion of **15** contained micelles with an average size of 168 nm (peak value) (Figure 4).

The zeta potential of the aqueous dispersion of **15** is -20.23 mV, which is in the expected range, in view of the hydroxyl groups of **15**. It can be assumed that in the aqueous dispersion the galactose block is on the surface of the micelles, whereas the PLA forms the core. Since the concentration of the stock solution cannot be determined unambiguously after dialysis, a different procedure was used for the evaluation of the critical micelle concentration (CMC). **15** was dissolved in DMSO followed by the addition of water. The CMC of **15** is $5.0 \mu\text{g mL}^{-1}$ as determined by dilution experiments and by DLS measurement

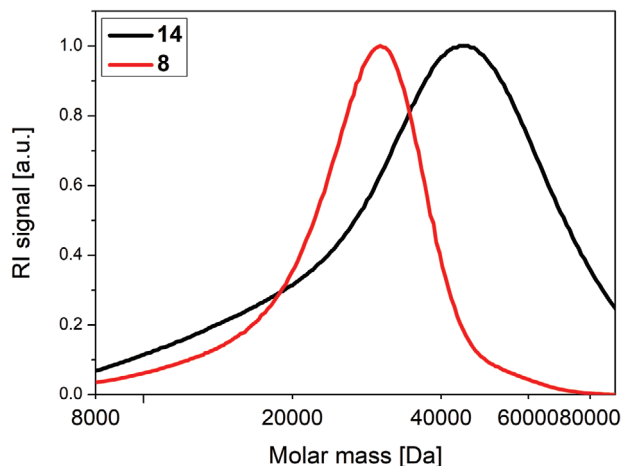


Figure 1. GPC measurement of **8** with an apparent number average molecular weight of $M_{n,app} = 24.000 \text{ g mol}^{-1}$ ($\bar{D} = 1.16$) in red and **14** with an apparent number average molecular weight of $M_{n,app} = 31.000 \text{ g mol}^{-1}$ ($\bar{D} = 1.42$) in black.

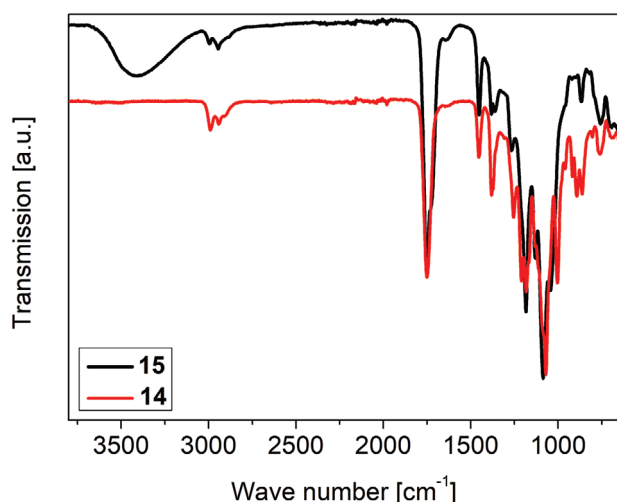


Figure 2. IR measurement of **14** in red and **15** in black.

(Figure S8, Supporting Information). Here, less than $0.5 \mu\text{L}$ of DMSO is dissolved per mL of water. It is already known that cosolvents like DMSO increase the CMC because they inhibit micelle formation.^[20] However, large deviations are only observed at higher concentrations of the cosolvent and can therefore be neglected.^[21] Remarkably, the hydrodynamic radius of the micelles decreased with reduced concentration above the CMC. For example, the micelles displayed an average diameter of 40 nm at a concentration of 0.25 mg mL^{-1} in water at 24°C . The CMC was too determined by fluorescence spectroscopy. The measurements support the results obtained with DLS (Figure S9, Supporting Information). The fluorescent dye used was 8-anilino-1-naphthalene-1-sulfonic acid (ANS). Similar results regarding the CMC of a dextran block copolymer with PLA in aqueous dispersion were reported by Zhao et al.^[22]

2.3. Deposition on Various Polymeric Surfaces

To investigate whether the micelles can interact with the surface of various polymers, dip model coating studies were carried out with film samples. For this purpose, an aqueous dispersion of **15** at a concentration of 2.5 mg mL^{-1} was prepared. Films of PLA, polypropylene (PP), perfluoroalkoxy (PFA), and polystyrene (PS) were immersed in the solution for dynamic coating. The dipping duration and frequency were varied. A new micelle dispersion was taken for each series to ensure the same micelle concentration. The samples were then dried for 24 h at room temperature (Figure S10, Supporting Information) and analyzed by contact angle measurement (Figure 5; Table S1, Supporting Information). A reference from polymer film was used for comparison.

With the PLA substrate, it is obvious that both the duration of dipping and the frequency are important. The longer the substrate is in solution, the thicker the layer of micelles on the surface becomes, which reduces the contact angle. The same effect is observed with the substrate PP, but it is less significant. PFA, which is a Teflon derivative, shows a different tendency. Here the contact angle is smaller for all samples than for the reference, but the longer and more frequently the substrate is dipped into the solution, the higher the contact angle becomes. The reason for this could be that the frequent immersion washes off the micelle layer. Since the surface of PFA has a very low surface tension, it is difficult to wet. With PS, on the other hand, all samples have a lower contact angle than the reference, but the frequency and duration of dipping do not change the contact angle (Figure S12, Supporting Information). It can be assumed that the surface of the substrate is saturated after a few seconds.

To investigate whether the surface of the substrate is permanently covered or dynamic, all samples were immersed in water for 24 h (Figure S11, Supporting Information). They were dried at room temperature for 24 h, and the contact angle was again measured (Figure 6; Table S2, Supporting Information). With the PLA substrate, the contact angles increased, but the surface was still covered by **15**. The trend from the previous measurement concerning the decreasing contact angle with an increased dipping duration and frequency remained. The reason for the permanent deposition is hydrogen bridges between the esters in the PLA backbone and the hydroxyl groups on the surface of the micelles. For all other substrates, the surface was no longer showing lower contact angles as compared to the reference samples (Figure S12, Supporting Information). This proves that the micelles are deposited on the surfaces by dipping the polymers in the aqueous micelle dispersion but do not interact with it.

2.4. Biological Degradation of **15**

To investigate the propensity of the galactose moieties in the produced block copolymers for metabolization by microbes, the bacteria strain *L. zeae* was used as model organism. This particular strain is known for its ability to metabolize a number of carbohydrates including galactose.^[23]

Growth of *L. zeae* in the presence of free galactose (20 g L^{-1}) as a C-source is shown in Figure 7A. The recorded culture triplicates show similar tendencies; initially, there is a lag phase of

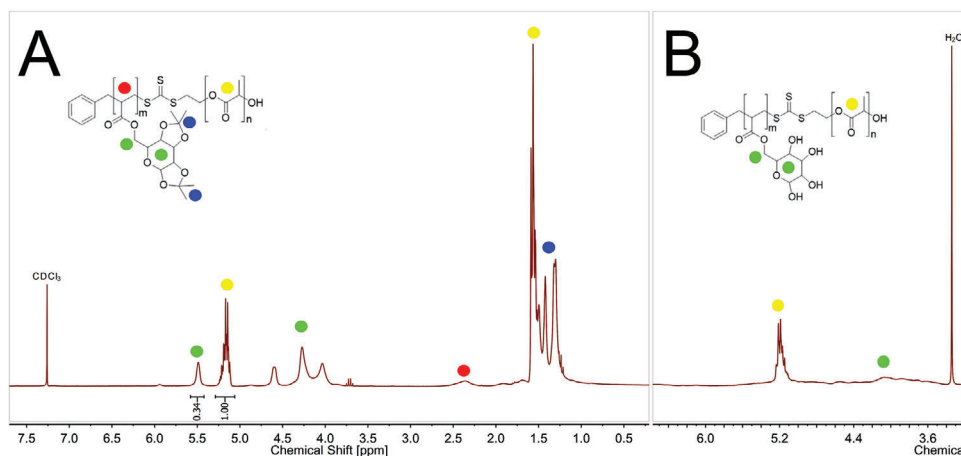


Figure 3. $^1\text{H-NMR}$ (300 MHz) of A) the protected polymer **14** measured in CDCl_3 and B) the deprotected **15** in DMSO.

Table 1. Data of thermal analysis measured by DSC and thermogravimetric analysis (TGA).

| Polymer | $T_{g1}^a)$ [°C] | $T_{g2}^a)$ [°C] | $T_{5\%}^b)$ [°C] | $T_{max}^b)$ [°C] |
|---------|---------------------|---------------------|----------------------|------------------------|
| 14 | 62 | 108 | 318 | 345, 433 |
| 15 | 55 | 152 | 210 | 71, 224, 280, 359, 409 |

^{a)} DSC: T_g values were determined from the second heating cycle (scanning rate = 50 K min^{-1} for **14** and 50 K min^{-1} for **15** under nitrogen); ^{b)} TGA: Temperature at 5% weight loss ($T_{5\%}$) was determined by TGA measurements at 10 K min^{-1} under nitrogen. T_{max} was determined from the first derivative of the TGA trace.

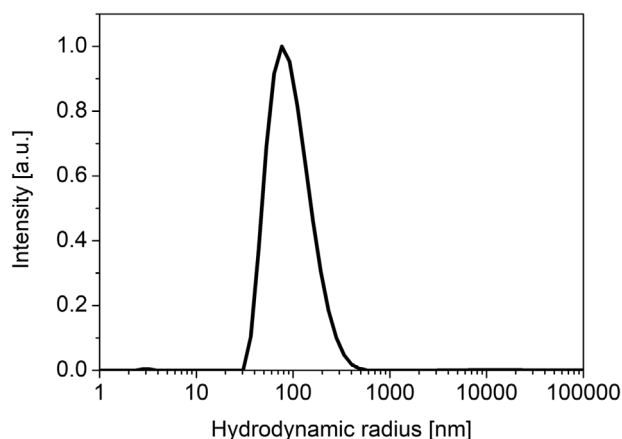


Figure 4. DLS measurement of **15** micelles in aqueous dispersion and a concentration of 2.5 mg mL^{-1} .

about 20 h, followed by an exponential growth phase lasting for another 45 h and reaching an OD_{600} of about 3, followed by a death phase. The average maximum growth rate, μ_{max} , in the exponential phase was 0.034 h^{-1} . By comparison, there was hardly any growth in just the basal medium lacking galactose as a C-source (Figure 7B).

When $\approx 20 \text{ g L}^{-1}$ of galactose was supplied via **15** to the basal medium, a similar growth behavior as in the presence of free galactose was typically seen, Figure 7C, albeit with a slightly lower

maximum growth rate (average μ_{max} : 0.018 h^{-1}). The duration of the growth phases in particular was similar. This could be an indication that access to the polymer-bound galactose was more difficult compared to free galactose. The nondecorated PLA backbone (**8**) alone, on the other hand, was also not able to support growth of *L. zeae* (Figure 7D); another indication is that indeed the galactose units of the block copolymer were serving as the C-source to the bacteria.

After the cultivation had been terminated, the rest of the sedimented polymer was recovered and cleaned by washing it several times with water before centrifugation. Subsequently, IR measurements were taken, which showed that the hydroxyl band at 3400 cm^{-1} was no longer in evidence (Figure 8). Obviously, the galactose moieties originally present in **15** had been neatly removed and consumed. The signals of PLA, on the other hand, were still recorded. So, significant biodegradation of these structures within the 100 h of cultivation had apparently not taken place.

For a more precise analysis of the structure, but also the quantities of remaining polymer blocks, $^1\text{H-NMR}$ spectra were, in addition, recorded (Figure 9). Again, no unprotected galactose moieties could be detected in the spectra of the residues recovered from the cultivations presented in Figure 7C. On the other hand, a small amount of **14** (protected galactose units) tends to remain in **15** after deprotection and evidence for this material was still found in the sediment. Obviously, the bacteria can metabolize the galactose moieties, but not **14**, due to the protective groups (Figure S13, Supporting Information). Moreover, the ratio between the protected galactose units and that of PLA remained the same (Figure S14, Supporting Information), supporting our assumption that the PLA block is not attacked by the bacteria.

Finally, the solubility behavior of the samples changed after cultivation. Although **15** could only be dissolved in DMSO, the sediment recovered post cultivation is soluble in chloroform as well. One possible reason for this is that the amphiphilicity of **15** was reduced during the cultivation with the bacterium *L. zeae*. In consequence, the resulting block copolymers are soluble in significantly more solvents.

Finally, attention should be drawn to the cultivation presented in Figure 10. For all practical means, this cultivation is an exact

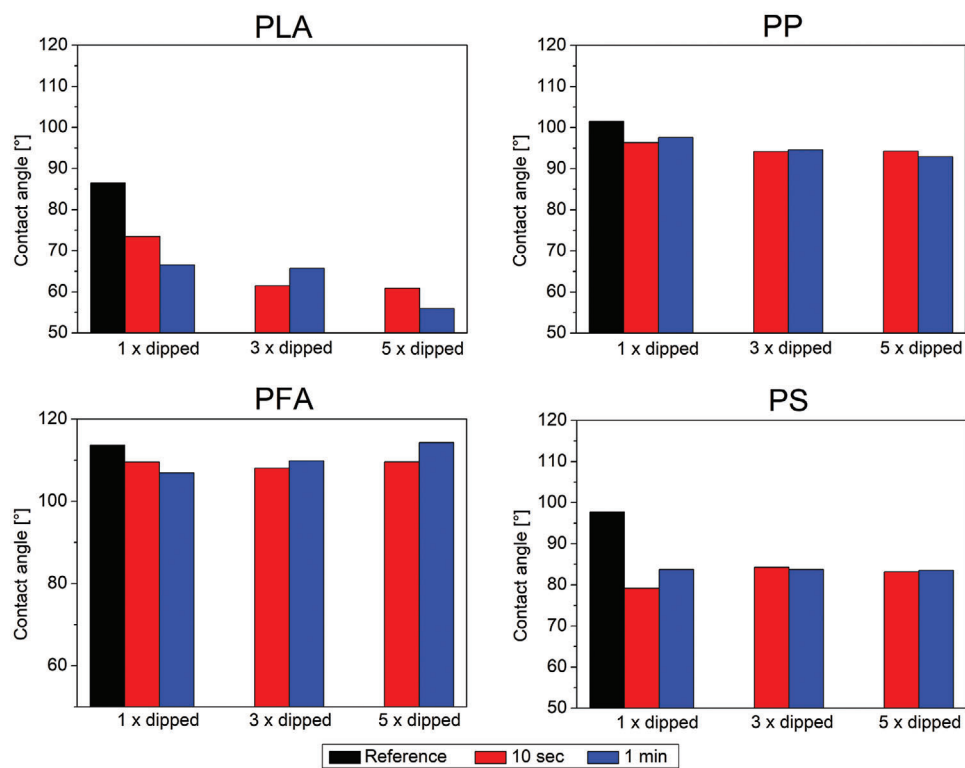


Figure 5. Contact angle of PLA, PP, PFA, and PS after dipping in the micelle solution for different times and quantities. The black column illustrates the contact angle of the substrates before dipping.

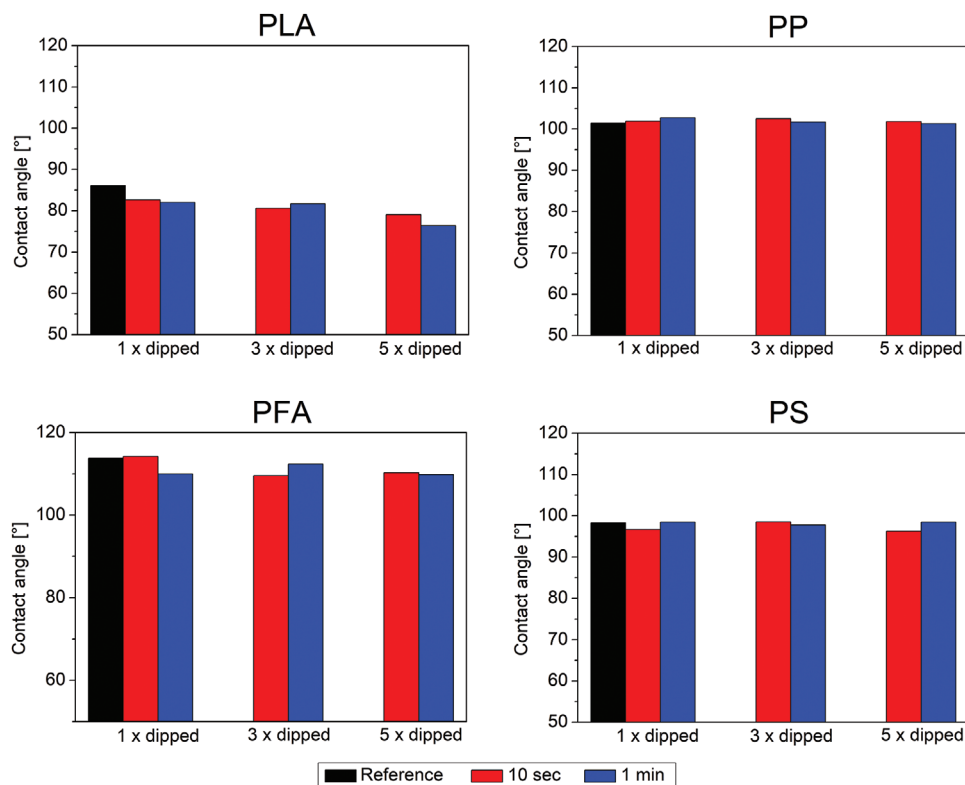


Figure 6. Contact angle of PLA, PP, PFA, and PS after removing the micelle layer by washing the surface with water for 24 h. The black column illustrates the contact angle of the substrates before dipping.

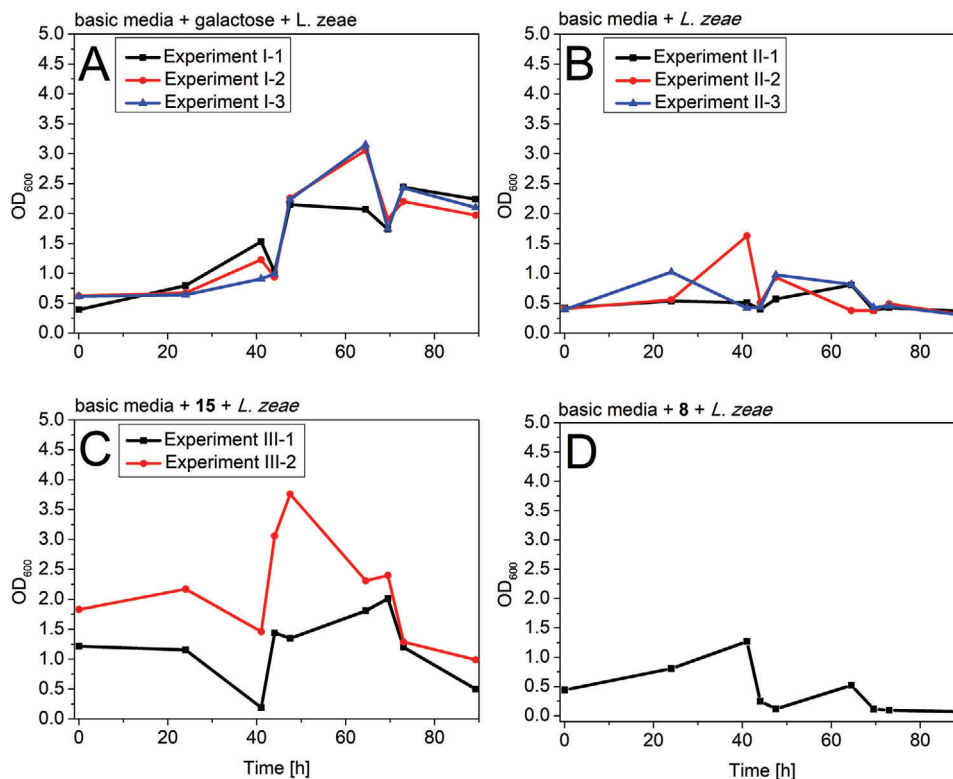


Figure 7. A) Growth curve of *L. zeae* in basic medium and galactose. B) Cultivation of *L. zeae* in basic medium. C) Cultivation of *L. zeae* in basic medium with 15. D) Cultivation of *L. zeae* in basic medium and 8. The measurement was only made once as a reference to prove if the higher OD₆₀₀ values caused due to the galactose in the polymer and not due to PLA. Panels (A)–(C) were prepared as triplicates. In panel (C) only two of the three triplicates were shown.

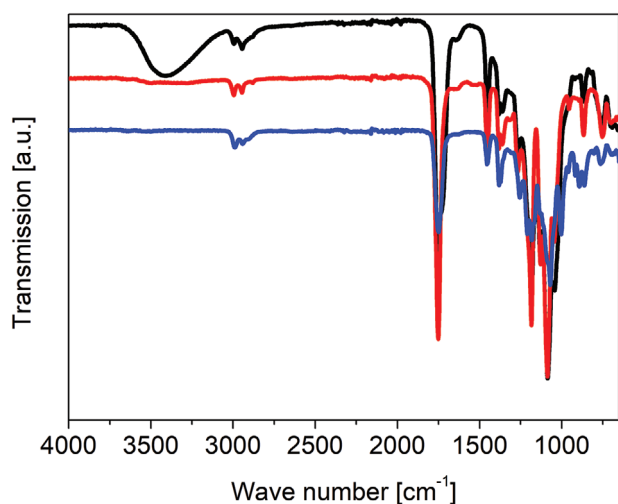


Figure 8. IR measurement of 15 before the biological single cultivation with *L. zeae* in black and afterward in red and blue.

replicate of the cultivations presented in Figure 7C, i.e., all experimental conditions were identical. However, the development of the OD₆₀₀ shows significant differences, while in the ¹H-NMR analysis (Figure 9) of the recovered material (Figure S15, Supporting Information), the protected galactose moieties are no longer detected. Signals corresponding to PLA are still in evidence, but

the amount of PLA found is an order of magnitude lower than in case of the previously discussed cultivations.

Contamination of the culture by other bacteria is unlikely, instead it can be speculated that the bacteria in this case succeeded in breaking down the polymer backbone, in particular the PLA blocks, perhaps thereby rendering the protected galactose moieties in 15 more accessible and making the lactic acid available for consumption. *Lactocaseibacillus zeae* is able to produce several esterases, which presumably are able to breakdown PLA structures.^[23] As far as we know, these esterases are produced as intracellular enzymes. However, their release, perhaps from dead cells, would constitute a considerable advantage for the general population when grown on sugar-decorated polymers.

3. Conclusion

In this study, the block copolymers 14 and the deprotected 15 were synthesized based on an efficient procedure for the educts. This enables synthesis at large scale, which opens completely new areas of application for these amphiphilic block copolymers. The polymers were analyzed by IR spectroscopy, ¹H-NMR spectroscopy, thermal analysis, and WAXS. It was shown that the synthesis leads to an amorphous amphiphilic block copolymer with galactose moieties. Based on these results, 15 was analyzed for its ability to form micelles in aqueous environment. DLS measurements and fluorescence spectroscopy indicated that micelles were formed and a CMC could be determined. As the concen-

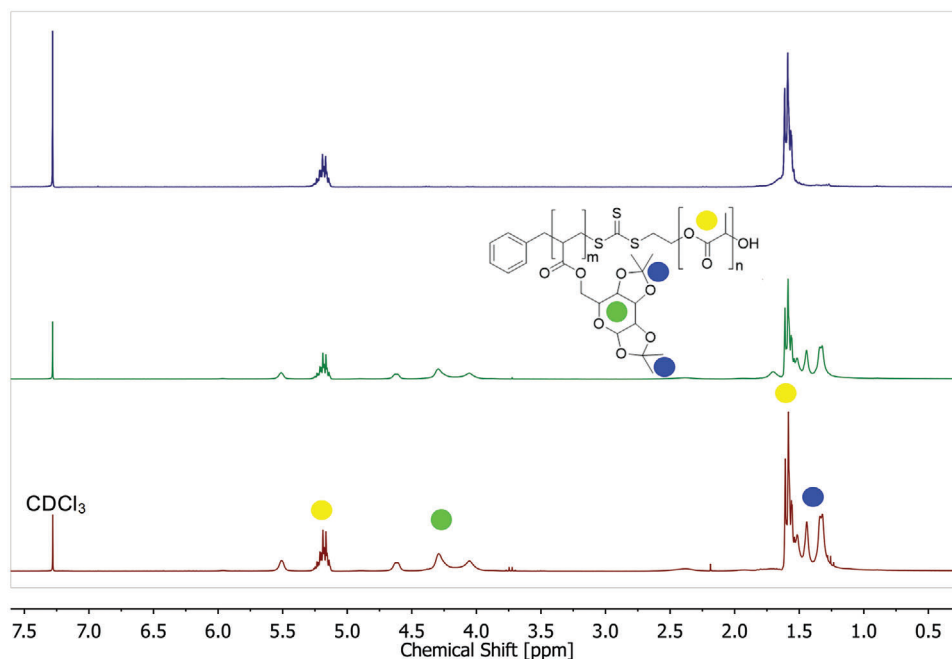


Figure 9. $^1\text{H-NMR}$ (300 MHz) of **14** in red and **15** after the single cultivation in green and blue. The sediment from the sample with a moderate OD_{600} is shown in green, and the sediment from the sample with an abnormal increase of the OD_{600} is visible in blue. The measurements were made in CDCl_3 .

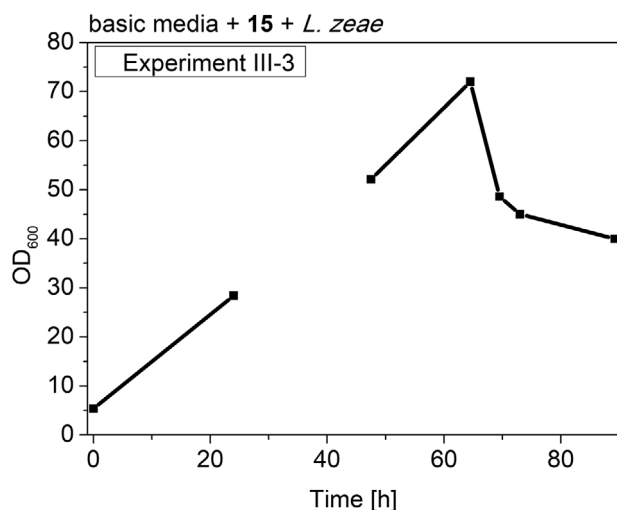


Figure 10. Cultivation of *L. zeae* in basic medium with **15**. Two points could not be measured (41 and 44 h) because the OD_{600} was too high.

tration of polymer in the solution decreases, the hydrodynamic radius of the micelles can also be reduced. Based on the negative zeta potential, it could be concluded that the galactose block of the amphiphilic block copolymer is on the surface of the micelle. Finally, contact angle measurements demonstrated that the synthesized polymer could be dip-coated onto the surfaces of various commercial polymers like PLA, PP, PFA, and PS by dynamic wetting. However, it was also shown that the coating can be washed off again by water. This showed that the polymers have a layer of micelles on them due to wetting with aqueous micelle solution. But there appears to be hardly any interaction between the polymers and the micelles, so they can be rinsed off. As known from

previous studies, the interaction of amphiphilic block copolymers with hydrophobic polymers or surfaces is restricted to hydrophobic block volume fraction and the length of the hydrophobic block.^[24] Only PLA can interact with the micelles due to hydrogen bonding between the ester groups in the backbone and the hydroxyl groups of the micelles. Due to the galactose residues in the polymer and the high surface area of micelles, the polymer shows a high attractiveness for microorganisms as demonstrated with the bacterium *L. zeae* as a model organism. In addition, IR and NMR spectroscopy showed that the galactose moieties can be metabolized by the bacteria. **15** was completely metabolized. Only **14** was found in the sediment, which remained as a negligible residue in **15** after deprotection. The next important step would be to use technical facilities such as composting plants or sewage treatment plants. The accelerated degradation of microplastic particles in the presence of **15** can then be investigated using the various microorganisms contained therein. In conclusion, the potential for coating of microplastic particles by sugar-block copolymers for the formation is given, but clearly further modifications on the block copolymers are required in order to fully exploit their potential for the microbial degradation of micro- and neoplastic plastic particles in aqueous environment. Upcoming investigation of the sugar-block copolymers will be performed with microorganisms, which are known to digest plastics.

4. Experimental Section

Materials: Mercaptoethanol was purchased from Merck, carbon disulfide, triethylamine, α,α,α -trifluorotoluene, AIBN, and benzylbromide were purchased from Sigma Aldrich. D,L-lactic acid was from Corbion Purac. 1,8-Diazobicyclo[5.4.0]undec-7-ene and the fluorescent dye 8-anilino-naphthalene-1-sulfonic acid were procured from TCI. 1,2:3,4-Di-O-

isopropylidene- α -D-galactopyranose was purchased from ABCR. Triethylamine and dichloromethane were dried over CaH_2 and distilled under protecting gas. Acryloyl chloride from Alfa Aesar was purified by condensation. AIBN was recrystallized three times in methanol. For biological cultivation tests, all materials were purchased from Grüssing GmbH or Carl Roth. *Lactocaseibacillus zaei* (DSMZ 20178) was purchased from German Collection of Microorganisms and Cell Cultures (DSMZ). The basic media for cultivation were modified after a previously published media composition:^[25] autoclaved Milli-Q water; peptone, 5 g L⁻¹; yeast extract, 5 g L⁻¹; K₂HPO₄, 5 g L⁻¹; and KH₂PO₄, 15 g L⁻¹. For precultivation, 20 g L⁻¹ of glucose was added. The other solvents and reagents were technical grade and used without further purification.

Methods: For the characterization of the polymers by differential scanning calorimetry a NETZSCH DSC 204 F1 Phoenix was used with aluminum crucibles from the company THEPRO. The evaluation was performed using the software Proteus 8.0.

The thermogravimetric analysis was done using a TG 209 F1 Libra thermobalance from NETZSCH. For evaluation of the data, the software Proteus 8.0 was used.

The structural characterization was done using a Bruker Avance 300 to record NMR spectra, with the chemical shift given in ppm and the coupling constant (J) in Hz. Deuterated chloroform, $\delta(\text{CDCl}_3) = 7.26$ ppm and $\delta(\text{DMSO}) = 2.50$ ppm, was used as the solvent. For the evaluation of the data, the software MestreNova was carried out.

The IR spectra were recorded with an EXCALIBUR SERIES, and the wavenumber was given in cm^{-1} . The samples were measured in a wavenumber region of 600–4000 cm^{-1} for four times. The data were evaluated with the software spectrum.

Polymer masses and dispersity were analyzed by gel permeations chromatography. The measurements were recorded using an SDV XL gel column (particle size = 5 μm with a separation range of 100–3000 000 Da) and a refractive index detector (1200 series, Agilent Technologies). Chloroform was used as the solvent and eluant with a flow rate of 0.5 mL min⁻¹. The calibration was performed with a narrowly distributed polystyrene homopolymer (PSS calibration kit). Before measurement, the sample was dissolved in chloroform and filtered with a 0.22 μm polytetrafluoroethylene (PTFE) filter. The injection volume was 20 μL . Toluene served as the internal standard.

WAXS measurements were done with a Bruker D8 ADVANCE with Cu K α radiation ($\lambda = 0.154$ nm). For the X-ray diffraction profiles, a transmission program in the 2θ angle range between 5° and 65° with a scanning speed of 0.05° min⁻¹ at 25 °C was used.

To form and characterize micelles, 250 mg of **15** was dissolved in 50 mL of DMSO for 30 min. Afterward, 50 mL of Milli-Q water was added dropwise under constant agitation to the solution. The mixture was dialyzed for 3 days with a water change every 12 h to remove the DMSO. For the formation of an aqueous micelle dispersion with a known concentration of 0.25 mg mL⁻¹, about 5 mg of **15** was dissolved in 0.5 mL of DMSO for 30 min. 19.5 mL of water was added dropwise under stirring. The obtained mixture was stirred for 2 h to allow for the formation of micelles. Afterward, the aqueous micelle dispersion was diluted until a concentration of 0.5×10^{-5} mg mL⁻¹ was obtained by 21 steps. The critical micelle concentration was determined by DLS and fluorescence spectroscopy. For DLS measurements, the laser intensity at an angle of 90° was detected. An ALV/DLS/SLS-5022GF system was used. As a photon-counting module, the ALV compact goniometer system, which consists of two high quantum efficiency avalanche photodiodes (QE APDs) for pseudo-cross correlation measurements, was used. A detector angle of 90°, a temperature of 294 K, and the cylindrical NeNe-laser wavelength at 632 nm (22 mW) were adjusted. To analyze the data, WINDOWS-95/98/NT-4.0 control and data reduction software was used. The CMC was also determined by fluorescence spectroscopy using a Jasco FP-8600 spectrofluorometer. The excitation wavelength was at 345 nm, measurements were done in a range between 380 and 600 nm. The sensitivity was adjusted to high. The fluorescent dye 8-anilino-naphthalene-1-sulfonic acid was dissolved in Milli-Q water (0.38×10^{-5} M) and used for the aqueous micelle dispersion. For dilution, only the ANS solution was utilized. The zeta potential was determined by laser Doppler anemometry using a Zetasizer NanoZS/ZEN3600

(Malvern Instruments, Herrenberg, Germany). The concentration of the aqueous micelle solution was 2.5 mg mL⁻¹, and the temperature while measuring was 25 °C. For calculation of the average zeta potential, the software DTS V 5.10 was used. All measurements were carried out three times.

For the dip coating and analysis by contact angle measurements, commercial PLA, PP, PVA, and PS films were cut into stripes and dipped into the aqueous micelle dispersion. For this, the dipping time was varied between 10 s and 1 min. Also, the dipping frequency was varied from one time over three times and five times. For every stripe, a new micelle solution was taken to avoid a concentration difference between the samples. The stripes were dried for 24 h in air. For the reference, the procedure was repeated. But instead of dipping in the micelle dispersion, the stripes were dipped in pure Milli-Q water to obtain a similar expiry. All samples were analyzed by contact angle measurements. Afterward, the micelle layer on the surface of the stripes was removed by washing the samples for 24 h in water before they were dried for 24 h in air. Then the contact angle was measured again. The measurements were done with a Krüss DSA 25 device. The images were taken with an Allied camera and analyzed with the computer program ADVANCE. The orientation was set to sessile drop, the fitting method to Young Laplace. Further settings were made with drop and a volume of 4 μL .

In the cultivation process, bacteria were precultivated at 37 °C and pH 6. Bacteria from the preculture (24 h, OD₆₀₀ at 2.3) were prepared for the following experiments: centrifuged at 13 000 rpm (Heraeus—BIOFUGE pico), discharging the supernatant, and bacteria were resuspended in 1 mL cultivation media—as described in the following. OD₆₀₀ was measured with Eppendorf BioPhotometer Plus.

For the experiments three triplicates were made: I) bacteria were cultivated in 3 \times : 5 mL basic media containing 1 mL of resuspended pre-culture and 20 g L⁻¹ of galactose. II) Bacteria were cultivated in 3 \times : 5 mL of basic media containing 1 mL of resuspended preculture. III) 3 \times each 500 mg of **15** was mixed with 4 mL of basic media and 1 mL of culture resuspended in basic media. With 500 mg of **15**, the galactose concentration in the media was at 20 g L⁻¹. Additionally, *L. zaei* was once cultivated in basic media containing pure PLA. Cultivation was about 90 h at 37 °C and pH 6; at the beginning during cultivation it was not regulated.

Synthesis: The synthesis of **5** was done by a procedure of Skey and O'reilly^[16] and was briefly described. **4** (13.59 g, 64 mmol, 1 eq.) was suspended in 100 mL of acetone. **1** (4.49 mL, 64 mmol, 1 eq.) was added and stirred for 10 min at room temperature before **2** (11.51 mL, 192 mmol, 3 eq.) was poured in the reaction mixture and stirred in for another 10 min. After **3** (7.61 mL, 64 mmol, 1 eq.) was introduced, the reaction mixture was stirred for 1 h. The resulting solid was filtered off and washed with acetone. Then the solvent was removed via a cold trap until a yellow, viscous mass remained. If impurities of the product are detected in the NMR, it can be purified via a column with hexane/ethyl acetate (3:1). (300 MHz, CDCl₃) = 7.31–7.22 (5H, m, Ph), 4.57 (2H, s, –S–CH₂–Ph), 3.82 (2H, t, OH–CH₂–), 3.55 (2H, t, –CH₂–S–CS–S–), 2.76 (1H, s, –OH).

In the synthesis of **8**, **6** (20 g, 138.8 mmol, 125 eq.) and **5** (0.27 g, 1.1 mmol, 1 eq.) were dissolved in 500 mL of dried dichloromethane at rt for 45 min. Afterward **7** (0.34 mL, 2.2 mmol, 2 eq.) was added and the reaction was stirred for 7 min. Then the polymerization was quenched by 160 mg of benzoic acid. After stirring for another 10 min, about half of the solvent was removed at the rotary evaporator. Then the polymer was precipitated in \approx 1.8 L cold pentane/EtOH (1.5 L/0.3 L). The precipitated polymer was transferred into cold EtOH and placed in the refrigerator for 1 h. After filtering off, the polymer, which was slightly yellowish, was dried in vacuo. The yield was 19 g (95%). (300 MHz, CDCl₃) = 5.14 (1H, m, –CH–), 1.56 (3H, s, –CH₃).

In the synthesis of **12**, **10** (40.0 g, 153.7 mmol, 1 eq.) and **11** (42.8 mL, 306.9 mmol, 2 eq.) were dissolved in 320 mL of dichloromethane (DCM) under protecting gas. The solution was cooled to 0 °C and **9** (27.4 mL, 337.8 mmol, 2.2 eq.) was added dropwise while the color of the solution turned to yellow. The ice bath was removed and the reaction mixture was stirred over night at rt. Afterward, the reaction mixture was washed with saturated sodium hydrogen carbonate solution and water, and the organic phase was dried over magnesium sulfate. Then the solvent was

removed completely by vacuum evaporation to obtain an orange/brown thick mass. The mass was dissolved in pentane, and the insoluble residue was filtered off before the solvent was completely removed again. The product was dried in vacuum to obtain a thick yellow mass. The yield was quantitative, and the product stored under protecting gas in the freezer until further use. (300 MHz, CDCl₃) = 6.39 (1H, d, =CH₂), 6.16 (1H, m, O-CO-CH=), 5.80 (1H, d, =CH₂), 5.52 (1H, d, -CH-), 4.60 (1H, m, -O-CH₂-CH-), 4.35–4.26 (4H, m, -CH-, -O-CH₂-CH-), 4.05 (1H, m, -CH-), 1.44 (6H, d, -CH₃), 1.32 (6H, d, -CH₃).

The synthesis of **14** was according to a procedure of Stenzel and co-workers.^[15] In brief, **12** (30.0 g, 95.4 mmol), **8** (10.0 g), and **13** (17.5 mg, 0.11 mmol) were added to 160 mL of trifluorotoluene and stirred until everything was dissolved and a clear, yellow solution resulted. Then the mixture was degassed for 20 min before it was heated to 70 °C for 6 h. The reaction was stopped in liquid nitrogen and the polymer was precipitated in cold pentane. Afterward, the polymer was filtered off and dissolved in dichloromethane before it was precipitated again in ethanol to remove any homopolymer formed during the reaction. After filtration the polymer, that is nearly white, was dried in vacuum. (300 MHz, CDCl₃) = 5.49 (0.34H, s, -CH_(sugar)-), 5.17 (1H, m, -CH_(PLA)-), 4.59 (0.37H, s, -O-CH₂-CH_(sugar)-), 4.27–4.03 (1.71H, m, -CH_(sugar)-), 2.35 (0.37H, s, -O-CO-CH-), 1.56 (3H, m, -CH_{3(PLA)}-), 1.42–1.30 (5.39H, m, -CH_{3(sugar)}-).

For deprotection, **14** (1.0 g, 3.23 mmol × 10⁻²) was heated in 33 mL of formic acid (90% in water) at 60 °C. After **14** was completely dissolved, the reaction mixture was stirred for 1 h at the same temperature. After cooling to room temperature, the reaction mixture was filled in a dialysis tube and dialyzed against Milli-Q water for 3 days with a water change every 8 h. Afterward, the polymer was dried in a freeze dryer to remove the water.

Supporting Information

Supporting Information is available from the Wiley Online Library or from the author.

Acknowledgements

This study was funded by the Deutsche Forschungsgemeinschaft (DFG, German Research Foundation) (Project No. 391977956-SFB 1357); Project C05. The authors gratefully acknowledge the use of equipment and assistance offered by the Keylab “Small Scale Polymer Processing” of the Bavarian Polymer Institute at the University of Bayreuth.

Open Access funding enabled and organized by Projekt DEAL.

Conflict of Interest

The authors declare no conflict of interest.

Data Availability Statement

The data that support the findings of this study are available in the supplementary material of this article.

Keywords

bacterial degradation, block copolymers, carbohydrates, micelles

Received: November 16, 2021

Revised: February 8, 2022

Published online:

- [1] a) R. Qi, D. L. Jones, Z. Li, Q. Liu, C. Yan, *Sci. Total Environ.* **2020**, 703, 134722; b) Q. Zhang, E. G. Xu, J. Li, Q. Chen, L. Ma, E. Y. Zeng,

- H. Shi, *Environ. Sci. Technol.* **2020**, 54, 3740; c) C. Laforsch, A. F. R. M. Ramsperger, S. Mondellini, T. S. Galloway, in *Regulatory Toxicology* (Eds: F. X. Reichl, M. Schwenk), Springer, Berlin **2021**, pp. 1–26; d) T. S. M. Amelia, W. M. A. W. M. Khalik, M. C. Ong, Y. T. Shao, H.-J. Pan, K. Bhubalan, *Prog. Earth Planet. Sci.* **2021**, 8, 12.
- [2] K. I. Jeyasanta, N. Sathish, J. Patterson, J. K. P. Edward, *Mar. Pollut. Bull.* **2020**, 154, 111055.
- [3] a) Y. Sun, C. Duan, N. Cao, X. Li, X. Li, Y. Chen, Y. Huang, J. Wang, *Sci. Total Environ.* **2021**, 806, 150516; b) C. Xu, B. Zhang, C. Gu, C. Shen, S. Yin, M. Aamir, F. Li, *J. Hazard. Mater.* **2020**, 400, 123228.
- [4] N. Meides, T. Menzel, B. Poetzschner, M. G. J. Löder, U. Mansfeld, P. Strohriegel, V. Altstaedt, J. Senker, *Environ. Sci. Technol.* **2021**, 55, 7930.
- [5] R. C. Thompson, Y. Olsen, R. P. Mitchell, A. Davis, S. J. Rowland, A. W. G. John, D. Mcgonigle, A. E. Russell, *Science* **2004**, 304, 838.
- [6] I. E. Napper, A. Baroth, A. C. Barrett, S. Bhola, G. W. Chowdhury, B. F. R. Davies, E. M. Duncan, S. Kumar, S. E. Nelms, Md. N. Hasan Niloy, B. Nishat, T. Maddalene, R. C. Thompson, H. Koldewey, *Environ. Pollut.* **2021**, 274, 116348.
- [7] H. K. Imhof, N. P. Ivleva, J. Schmid, R. Niessner, C. Laforsch, *Curr. Biol.* **2013**, 23, R867.
- [8] a) J.-J. Guo, X.-P. Huang, L. Xiang, Y.-Z. Wang, Y.-W. Li, H. Li, Q.-Y. Cai, C.-H. Mo, M.-H. Wong, *Environ. Int.* **2020**, 137, 105263; b) B. Xu, F. Liu, Z. Cryder, D. Huang, Z. Lu, Y. He, H. Wang, Z. Lu, P. C. Brookes, C. Tang, J. Gan, J. Xu, *Environ. Sci. Technol.* **2020**, 50, 2175.
- [9] a) Y. Zhang, S. Kang, S. Allen, D. Allen, T. Gao, M. Sillanpää, *Earth-Sci. Rev.* **2020**, 203, 103118; b) H. Yang, Y. He, Y. Yan, M. Junaid, J. Wang, *J. Nanomater.* **2021**, 11, 2747.
- [10] a) T. K. Dey, Md. E. Uddin, M. Jamal, *Environ. Sci. Pollut. Res. Int.* **2021**, 28, 16925; b) M. Padervand, E. Lichtfouse, D. Robert, C. Wang, *Environ. Chem. Lett.* **2020**, 18, 807; c) T. Poerio, E. Piacentini, R. Mazzei, *Molecules* **2019**, 24, 4148.
- [11] A. Paço, K. Duarte, J. P. Da Costa, P. S. M. Santos, R. Pereira, M. E. Pereira, A. C. Freitas, A. C. Duarte, T. A. P. Rocha-Santos, *Sci. Total Environ.* **2017**, 586, 10.
- [12] S. Yoshida, K. Hiraga, T. Takehana, I. Taniguchi, H. Yamaji, Y. Maeda, K. Toyohara, K. Miyamoto, Y. Kimura, K. Oda, *Science* **2016**, 351, 1196.
- [13] S. Shabbir, M. Faheem, N. Ali, P. G. Kerr, L.-F. Wang, S. Kuppusamy, Y. Li, *Sci. Total Environ.* **2020**, 717, 137064.
- [14] N. F. Zaaba, M. Jaafar, *Polym. Eng. Sci.* **2020**, 60, 2061.
- [15] S. R. S. Ting, A. M. Gregory, M. H. Stenzel, *Biomacromolecules* **2009**, 10, 342.
- [16] J. Skey, R. K. O'reilly, *Chem. Commun.* **2008**, 4183.
- [17] A. Gregory, M. H. Stenzel, *Prog. Polym. Sci.* **2012**, 37, 38.
- [18] M. Piccini, D. J. Leak, C. J. Chuck, A. Buchard, *Polym. Chem.* **2020**, 11, 2681.
- [19] A. Kumar, A. R. Weig, S. Agarwal, *Macromol. Mater. Eng.* **2021**, 2100602.
- [20] V. Sharma, P. Cantero-López, O. Yañez-Osses, A. Kumar, *J. Chem. Eng. Data* **2018**, 63, 3083.
- [21] H. Aizawa, *J. Appl. Crystallogr.* **2010**, 43, 630.
- [22] Z. Zhao, Z. Zhang, L. Chen, Y. Cao, C. He, X. Chen, *Langmuir* **2013**, 29, 13072.
- [23] C.-H. Huang, C.-C. Chen, J.-S. Liou, A.-Y. Lee, J. Blom, Y.-C. Lin, L. Huang, K. Watanabe, *Int. J. Syst. Evol. Microbiol.* **2020**, 70, 3755.
- [24] a) Y. Chen, G. Wulff, *Macromol. Chem. Phys.* **2001**, 202, 3273; b) G. E. Parkes, H. J. Hutchins-Crawford, C. Bourdin, S. Reynolds, L. J. Leslie, M. J. Derry, J. L. Harries, P. D. Topham, *Polym. Chem.* **2020**, 11, 2869.
- [25] W. Sabra, D. Dietz, A. P. Zeng, *Appl. Microbiol. Biotechnol.* **2013**, 97, 5771.